

## Flash K-alpha radiography of laser-driven solid sphere compression for fast ignition

P. K. Patel

March 30, 2016

**Applied Physics Letters** 

## Disclaimer

This document was prepared as an account of work sponsored by an agency of the United States government. Neither the United States government nor Lawrence Livermore National Security, LLC, nor any of their employees makes any warranty, expressed or implied, or assumes any legal liability or responsibility for the accuracy, completeness, or usefulness of any information, apparatus, product, or process disclosed, or represents that its use would not infringe privately owned rights. Reference herein to any specific commercial product, process, or service by trade name, trademark, manufacturer, or otherwise does not necessarily constitute or imply its endorsement, recommendation, or favoring by the United States government or Lawrence Livermore National Security, LLC. The views and opinions of authors expressed herein do not necessarily state or reflect those of the United States government or Lawrence Livermore National Security, LLC, and shall not be used for advertising or product endorsement purposes.

Flash  $K\alpha$  radiography of laser-driven solid sphere compression for Fast Ignition

H. Sawada<sup>1</sup>, S. Lee<sup>2</sup>, T. Shiroto<sup>3</sup>, H. Nagatomo<sup>2</sup>, Y. Arikawa<sup>2</sup>, H. Nishimura<sup>2</sup>, T. Ueda<sup>2</sup>, K. Shigemori<sup>2</sup>, A. Sunahara<sup>4</sup>, N. Ohnishi<sup>3</sup>, F. N. Beg<sup>5</sup>, W. Theobald<sup>6</sup>, F. Pérez<sup>7</sup>, P. K. Patel<sup>8</sup> and S. Fujioka<sup>2</sup>

- 1. Department of Physics, University of Nevada Reno, USA
- 2. Institute of Laser Engineering, Osaka University, Japan
- 3. Department of Aerospace Engineering, Tohoku University, Japan
- 4. Institute of Laser Technology, Japan
- 5. University of California San Diego, USA
- 6. Laboratory for Laser Energetics, University of Rochester, USA
- 7. LULI, Ecole Polytechnique, France
- 8. Lawrence Livermore National Laboratory, USA

## **Abstract**

Time-resolved compression of a laser-driven solid deuterated plastic (CD) sphere with a cone was measured with flash  $K\alpha$  x-ray radiography. A spherically converging shockwave launched by nanosecond GEKKO XII beams was used for compression while a flash of 4.51 keV Ti  $K\alpha$  x-ray backlighter was produced by a high-intensity, picosecond laser LFEX near peak compression for radiography. Areal densities of the compressed core were inferred from two-dimensional backlit x-ray images recorded with a narrow-band spherical crystal imager. The maximum areal density in the experiment was estimated to be  $81 \pm 26$  mg/cm<sup>2</sup>. The temporal evolution of the experimental and simulated areal densities with a 2-D radiation-hydrodynamics code is in good agreement.

X-ray radiography using nanosecond-laser-produced plasma sources is a widely used powerful diagnostic technique to image detailed structures of laser- or x-ray driven objects such as laser-driven implosion, radiative shocks and growths of hydrodynamic instability. [1,2] In particular, the 2-D projected radiographs can provide information of its density profile with knowledge of the backlighter x-ray spectrum and a symmetric assumption. Since quasi-monochromatic, thermal x-ray emission lasts over nanoseconds, time-resolved measurements are achieved by detectors with a  $\sim$  40 ps gating time [3,4]. Diagnosing faster plasma evolution such as stagnation processes of laser-driven implosion requires a few picoseconds temporal resolution.

Generation of a flash, bright, monochromatic x-ray has been studied using high-intensity (I >  $10^{17}$  W/cm<sup>2</sup>), picosecond lasers irradiating on a metal foil target [5]. With femtosecond lasers, the pulse duration of femtosecond K $\alpha$  sources has been systematically studied using analytical and numerical models. [6] Experimentally, the pulse of characteristic Cu K $\alpha$  x-ray produced by a 10 ps, kilojoule OMEGA EP laser has been measured with an ultrafast streak camera to be ~ 12 ps, similar to the order of the laser pulse duration. [7] By combining such a short-pulse x-ray source with a spherically bent Bragg crystal, high spatiotemporal, narrow-band spherical crystal imagers have been developed [8, 9] and applied for recording radiographs of spherical implosions by lasers [10,11,12] or x-rays [13] as well as studying the transport of fast electrons in a dense plasma [14]. In backlighting experiments, the backlighter brightness must be

substantially higher than the self-emission of the implosion because the ratio of those signals essentially sets the limit of the range of core densities to be inferred.

In this Letter, we present time-resolved compression measurements of laser-driven solid deuterated plastic (CD) sphere with flash Ti K\alpha radiography using a newly completed highenergy, Petawatt laser LFEX [15]. The main focus of this work is to benchmark a twodimensional radiation hydrodynamics code that will be used for designing fast ignition targets against experimentally inferred areal densities. This allows us to develop an experimental and computational platform for testing production of a high areal density fusion fuel with a solid sphere. The use of the solid sphere provides primarily three advantages over a shell implosion: negligible Rayleigh-Taylor (RT) instability growths [16] during the compression, no self emission due to the shell stagnation and a slow fuel assembly time. For fast ignition (FI) [17, 18], the formation of a high temperature hot spot is unnecessary unlike a conventional central hot spot ignition scheme where the stagnation of a fast imploding shell creates a high temperature spark surrounded by a dense fuel layer [19,20,21]. Instead, ignition is achieved by the injection of an additional intense laser into the dense fuel. The fuel assembly for FI, thus, can be designed with a thick shell capsule [22] or a solid sphere [23], insusceptible to the growths of the RT instability, as long as the core areal density is sufficiently high enough for deposition of charged particle beams (electrons, protons or ions). Our simulation predicts ~ 330 ps (in FWHM) fuel assembly time for a sphere compression compared to 80 ps for a shell compression. This slow compression relaxes the tolerance of the timing itter error originated in the electrical signal synchronization between the compression and the backlighter lasers for radiography.

The experiment was carried out at Institute of Laser Engineering using the high-energy, petawatt LFEX laser [15] and the GEKKO XII (GXII) nano-second laser [24]. A 200 µm diameter solid CD sphere ( $\rho = 1.1 \text{ g/cm}^3$ ) was attached on the tip of an Au cone having 45° full opening angle, 100 µm inner tip diameter, 17 µm cone tip thickness and 10 µm wall thickness. The cone was coated outside with 17 µm thick CH layer to prevent it from direct laser irradiation. The sphere was irradiated by 9 GXII beams with the total energy of ~ 2.7 kJ (~300J/beam). The drive laser pulse measured with an oscilloscope was characterized by fitting two Gaussian profiles (0.9 ns + 1.45 ns FWHM before and after the peak) and fed into simulations. 4.51 keV K\alpha x-ray was produced by the 1.6 ps, 1000 J LFEX beam irradiating on a Ti foil around the time of the peak compression. The x-ray transmitted through the compressed target was imaged with a spherically bent quartz crystal on to an imaging plate (IP) detector.[25] The crystal imager had a magnification of 11.5,  $12.5 \pm 2.5 \mu m$  spatial resolution and  $\sim 5 \text{ eV}$ spectral resolution. No K\alpha pulse measurement was performed in this experiment, but according to the theoretical prediction [6], it is reasonable to assume that the duration of the x-ray pulse is of the order of the short-pulse laser of 1.6 ps, enabling to record an instantaneous image of the compressing sphere.

The relative timing of the backlighter x-ray with respect to the compression lasers was recorded with a heavily shielded x-ray streak camera [26,27,28]. Figure 1 shows a measured streaked image and temporal lineouts. The streak camera was fielded to record side-on corona emission with the slit orientation along the cone axis. The recorded image shows both the corona emission from the CD sphere and x-ray emission from the Au cone as well as hard x-ray signals produced by the LEFX laser-target interaction. Note that the LFEX x-ray on the streak was produced by the direct incidence of the hard x-ray on the photocathode and it does not represent its duration. Figure 1 (c) shows the lineouts along the Au emission and the LFEX-induced signals. In this experiment, the peak of the Gaussian pulse was chosen to be 4.0 ns as the

reference timing. The streak timing was determined by matching the leading edge of the Au emission profile to the measured laser profile. The timing of the LFEX laser of  $4.17 \pm 0.043$  ns on this shot was estimated from the delay between the laser peak and the peak of the hard x-ray emission that indicates the direct hit of the hard x-ray. The error was based on the camera temporal resolution and the uncertainty of the fit to the Au emission. Both streaked and radiograph images were recorded on every shots for systematically estimating the radiograph timing.

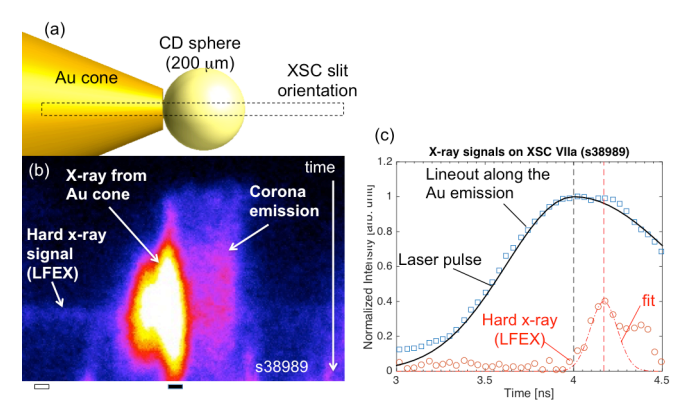


Figure 1 (a) A model view of the cone-sphere target from the x-ray streak camera and its slit orientation. (b) A measured x-ray streak image (s38989). (c) Space-averaged emission profiles from the Au cone and the LFEX hard x-ray. The open and filled bars at the bottom of the streak image indicate the width of the averaged spatial extents.

Figure 2 (a) shows a raw radiograph image of a driven cone-sphere target. The formation of a dense core was observed in front of the cone tip only when it was driven. From the sharpness of the shadow of the Au cone edge, the spatial resolution was estimated to be  $12.5 \pm 2.5$  µm corresponding to 6 pixels. The experimental optical depth profile was obtained in the following steps. After smoothing the image with a Gaussian filter to take the spatial resolution into account, bremsstrahlung background signal produced by LFEX, which was measured through the Au cone, was uniformly subtracted. The unattenuated intensity profile  $I_0$  is then obtained by using a surface fit outside the core and cone to the emission from the Ti foil. Optical depth is calculated using the relation,  $\tau = -\log(I/I_0)$ , where I and  $I_0$  are the measured and extrapolated intensity profiles. Fig. 2(b-d) shows the 2-D optical depths at 4.11, 4.17 and 4.38 ns. The images clearly show assemblies of high density plasma well separated from the cone tip. Although the first two images are noisy, particularly high values in optical depth can be found near the plasma center. Fig. 2(e) shows the radial profiles of the vertical lineouts at the center of the optical depth contours. The sizes of the core plasma are within 50 µm in radius for all three shots while the profile at 4.17 ns is higher than others. The vertical lineouts were split in top and bottom half, and both radial profiles were independently inverted using Fourier-based Abel inversion [29] to reconstruct axisymmetric density profiles,  $\rho(r)$ . The reconstructed optical depth profiles from the inverted images were compared to the measured for estimating the reconstruction error. By integrating the density distribution and averaging oRs from two profiles obtained from each side, the experimental pR was calculated and compared later with results of hydrodynamic simulations.

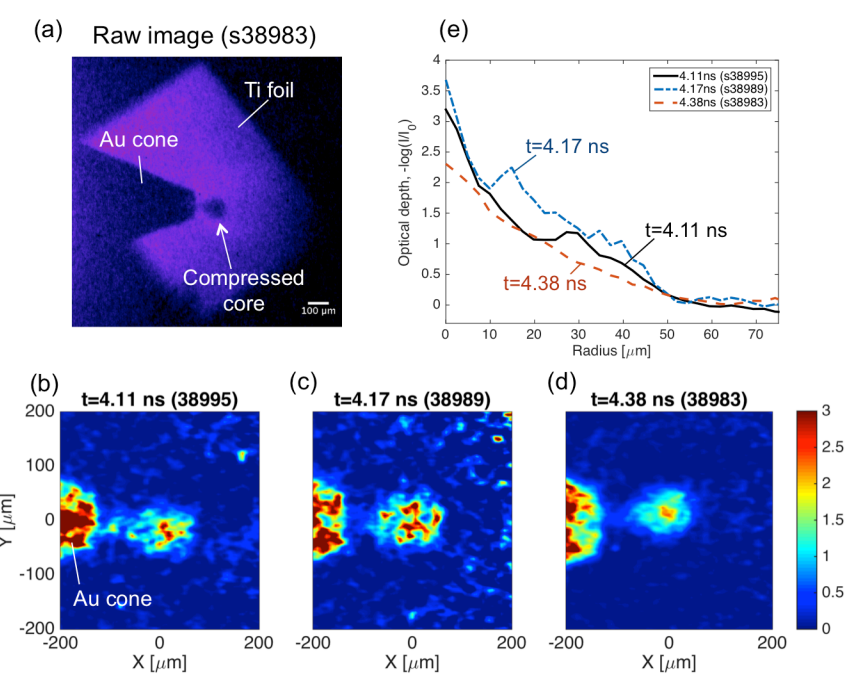


Figure 2 (a) Raw radiograph image (s38983). Experimental optical depth profiles (b) t = 4.11 ns (s38995), (c) t = 4.17 ns (s38989) and (d) t = 4.38 ns (s38995). (e) Azimuthal averaged radial profiles of the core shown in (b), (c) and (d).

Compression of the laser-driven cone-sphere target was simulated with an axisymmetric twodimensional radiation hydrodynamics code RAICHO [30] using the experimental laser and target specification. The numerical scheme is based on the finite volume method with the Eulerian mesh. Laser absorption via inverse bremsstrahlung is handled with one-dimensional ray tracing over the radial direction. The equations for the radiation transfer and thermal conduction are parabolized using a flux limited model (f=0.06) and neglecting any non-local effects. The opacity of the target materials is included using tabulated data based on average-ion model assuming collisional radiative equilibrium. The equations of state for the high-density plasma were composed by the theory developed by More et al [31]. Figure 3 shows simulated 2-D mass density and temperature contours smoothed with the experimental resolution. The temperature and density variations in the azimuthally averaged radial profile within the core are used to estimate variations in calculated opacity. Simulated areal density was calculated by integrating the core density distribution in the direction perpendicular to the cone. The sphere compression was also modeled with 1-D rad-hydro code, Helios [32], assuming no cone attached to the target. The comparison between the 1-D and 2-D simulations provides a quantitative estimation of the effects of radiation from the Au cone and asymmetric laser irradiation on the compression.

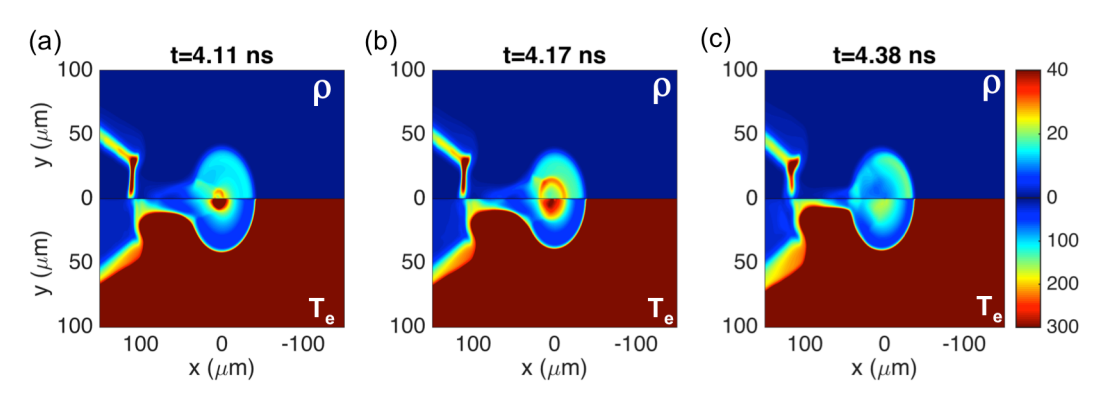


Figure 3 Simulated mass density ( $\rho$ ) and electron temperature ( $T_e$ ) contours for (a) t= 4.11 ns (s38995), (b) t=4.17 ns (s38989) and (c) t=4.38 ns (s38995).

Figure 4 compares the experimental areal densities with the 1-D and 2-D simulation results along with the laser pulse shape. The experimental data agree with the 2-D simulation well. The 1-D simulation predicts faster decompression than the 2-D, which disagree with the data. The experimental uncertainties are attributed to the background subtraction and division by the extrapolated intensity distribution in obtaining optical depth (9%, 11% and 6%), the Abel inversion process (13%, 25% and 8%), and variations in the calculated mass absorption coefficient (10%, 10% and 8%). The inferred  $\rho$ Rs with the overall errors are 72 ± 13 mg/cm<sup>2</sup> (±19%), 87 ± 26 mg/cm<sup>2</sup> (±29%) and 51 ± 7 mg/cm<sup>2</sup> (±13%) at t=4.11, 4.17 and 4.38 ns, respectively. The comparison shows that a 2-D simulation including radiation from the Au cone and asymmetric laser irradiation is required to model the full temporal evolution of the areal density.

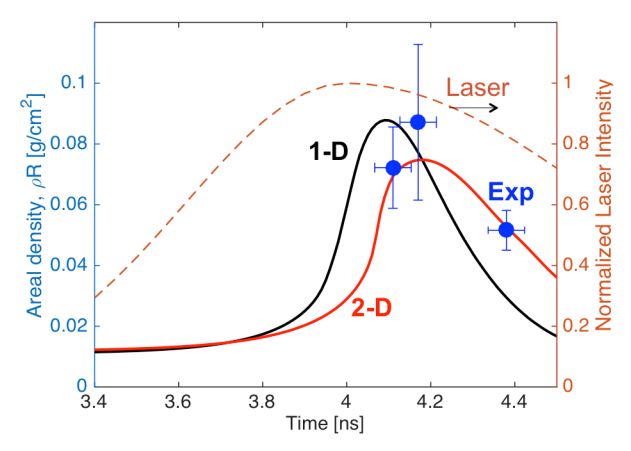


Figure 4 A comparison of the experimental and calculated areal densities. The simulations were performed in 2-D cylindrical geometry for the cone-sphere target and in 1-D for spherical symmetric compression.

In conclusion, time-resolved compression of laser-driven solid CD sphere with a cone was measured with flash  $K\alpha$  x-ray radiography. The temporal evolution of the experimental  $\rho$ Rs deduced from the radiograph images agree with the 2-D simulation. The benchmarked numerical code will be used to improve a design of high areal density fuel assembly for fast ignition.

## (Acknowledgement)

This work was performed with the support and under the auspices of the NIFS Collaboration Research program (NIFS13KUGK072). The authors would like to thank the crews for the GXII and LFEX laser operation and the experimental group. H.S acknowledged the support by the UNR International Activities Grant.

<sup>&</sup>lt;sup>1</sup> O.L. Landen, D.R. Farley, S.G. Glendinning, L.M. Logory, P.M. Bell, J.A. Koch, F.D. Lee, D.K. Bradley, D.H. Kalantar, C.A. Back, and R.E. Turner, Rev. Sci. Instrum. 72, 627 (2001).

<sup>&</sup>lt;sup>2</sup> B.A. Remington, J. Kane, R.P. Drake, S.G. Glendinning, K. Estabrook, R. London, J. Castor, R.J. Wallace, D. Arnett, E. Liang, R. McCray, A. Rubenchik, and B. Fryxell, Phys. Plasmas 4, 1994 (1997).

<sup>&</sup>lt;sup>3</sup> F.J. Marshall, P.W. McKenty, J. a. Delettrez, R. Epstein, J.P. Knauer, V. a. Smalyuk, J. a. Frenje, C.K. Li, R.D. Petrasso, F.H. Séguin, and R.C. Mancini, Phys. Rev. Lett. 102, 1 (2009).

<sup>&</sup>lt;sup>4</sup> H. Shiraga, H. Nagatomo, W. Theobald, A. A. Solodov, and M. Tabak, Nucl. Fusion **54**, 054005 (2014).

<sup>&</sup>lt;sup>5</sup> H.S. Park, D.M. Chambers, H.K. Chung, R.J. Clarke, R. Eagleton, E. Giraldez, T. Goldsack, R. Heathcote, N. Izumi, M.H. Key, J. A. King, J. A. Koch, O.L. Landen, A. Nikroo, P.K. Patel, D.F. Price, B. A. Remington, H.F. Robey, R. A. Snavely, D. a. Steinman, R.B. Stephens, C. Stoeckl, M. Storm, M. Tabak, W. Theobald, R.P.J. Town, J.E. Wickersham, and B.B. Zhang, Phys. Plasmas 13, (2006).

<sup>&</sup>lt;sup>6</sup> C. Reich, P. Gibbon, I. Uschmann, and E. Forster, Phys. Rev. Lett. 84, 4846 (2000).

<sup>&</sup>lt;sup>7</sup> P.M. Nilson, J.R. Davies, W. Theobald, P. A. Jaanimagi, C. Mileham, R.K. Jungquist, C. Stoeckl, I. A. Begishev, A. A. Solodov, J.F. Myatt, J.D. Zuegel, T.C. Sangster, R. Betti, and D.D. Meyerhofer, Phys. Rev. Lett. 108, 085002 (2012).

<sup>&</sup>lt;sup>8</sup> J.A. King, K. Akli, R. A. Snavely, B. Zhang, M.H. Key, C.D. Chen, M. Chen, S.P. Hatchett, J. A. Koch, A.J. MacKinnon, P.K. Patel, T. Phillips, R.P.J. Town, R.R. Freeman, M. Borghesi, L. Romagnani, M. Zepf, T. Cowan, R. Stephens, K.L. Lancaster, C.D. Murphy, P. Norreys, and C. Stoeckl, Rev. Sci. Instrum. 76, 076102 (2005).

<sup>9</sup> C. Stoeckl, G. Fiksel, D. Guy, C. Mileham, P.M. Nilson, T.C. Sangster, M.J. Shoup, and W. Theobald, Rev. Sci. Instrum. 83, 033107 (2012).

<sup>&</sup>lt;sup>10</sup> J.A. King, K. Akli, B. Zhang, R.R. Freeman, M.H. Key, C.D. Chen, S.P. Hatchett, J.A. Koch, A.J. MacKinnon, P.K. Patel, R. Snavely, R.P.J. Town, M. Borghesi, L. Romagnani, M. Zepf, T. Cowan, H. Habara, R. Kodama, Y. Toyama, S. Karsch, K. Lancaster, C. Murphy, P. Norreys, R. Stephens, and C. Stoeckl, Appl. Phys. Lett. 86, 191501 (2005).

<sup>(2005).

11</sup> W. Theobald, A. A. Solodov, C. Stoeckl, K.S. Anderson, F.N. Beg, R. Epstein, G. Fiksel, E.M. Giraldez, V.Y. Glebov, H. Habara, S. Ivancic, L.C. Jarrott, F.J. Marshall, G. McKiernan, H.S. McLean, C. Mileham, P.M. Nilson, P.K. Patel, F. Pérez, T.C. Sangster, J.J. Santos, H. Sawada, a. Shvydky, R.B. Stephens, and M.S. Wei, Nat. Commun. 5, 5785 (2014).

<sup>&</sup>lt;sup>12</sup> H. Sawada, F. Pérez, A. A. Solodov, W. Theobald, F. N. Beg, V. Glebov, L. C. Jarrott, A. J. Kemp, M. H. Key, H. S. McLean, R. B. Stephens, C. Stoeckl, M. S. Wei and P. K. Patel, submitted to Physics of Plasmas (2016)

<sup>&</sup>lt;sup>13</sup> D.T. Casey, D.T. Woods, V.A. Smalyuk, O.A. Hurricane, V.Y. Glebov, C. Stoeckl, W. Theobald, R. Wallace, A. Nikroo, M. Schoff, C. Shuldberg, K.J. Wu, J.A. Frenje, O.L. Landen, B.A. Remington, and G. Glendinning, Phys. Rev. Lett. 114, 205002 (2015).

<sup>&</sup>lt;sup>14</sup> L.C. Jarrott, M.S. Wei, C. McGuffey, A.A. Solodov, W. Theobald, B. Qiao, C. Stoeckl, R. Betti, H. Chen, J. Delettrez, T. Doppner, E.M. Giraldez, V.Y. Glebov, H. Habara, T. Iwawaki, M.H. Key, R.W. Luo, F.J. Marshall, H.S. McLean, C. Mileham, P.K. Patel, J.J. Santos, H. Sawada, R.B. Stephens, T. Yabuuchi, and F.N. Beg, Nat Phys advance on, (2016).

<sup>&</sup>lt;sup>15</sup> N.Miyanaga, H. Azechi, K.A. Tanaka, T. Kanabe et al., J. dePhysique IV 133, 81 (2006)

<sup>&</sup>lt;sup>16</sup> S. E. Bodner, Phys. Rev. Lett. 33, 761 (1974)

<sup>&</sup>lt;sup>17</sup> M. Tabak, J. Hammer, M. E. Glinsky, W. L. Kruer, S. C. Wilks, J. Wood- worth, E. M. Campbell, M. D. Perry, and R. J. Mason, Phys. Plasmas 1, 1626 (1994).

<sup>&</sup>lt;sup>18</sup> R. Kodama, P. A. Norreys, K. Mima, A. E. Dangor, R. G. Evans, H. Fujita, Y. Kitagawa, K. Krushelnick, T.Miyakoshi, N.Miyanaga, T. Norimatsu, S. J. Rose, T. Shozaki, K. Shigemori, A. Sunahara, M. Tampo, K. A. Tanaka, Y. Toyama, T. Yamanaka, andM. Zepf, Nature 412, 798–802 (2001).

<sup>&</sup>lt;sup>19</sup> J. H. Nuckolls , L. Wood , A. Thiessen , and G. B. Zimmerman, Nature (London) 239, 139 (1972).

<sup>24</sup> C. Yamanaka, Y. Kato, Y. Izawa, T. Yamanaka, T. Sasaki, M. Nakatsuka, T. Mochizuki, J. Kuroda, and S. Nakai, IEEE J. Quantum Electron. QE- 17, 1639 (1981);

<sup>25</sup> H. Sawada, S. Fujioka, T. Hosoda, Z. Zhang, Y. Arikawa, H. Nagatomo, H. Nishimura, A. Sunahara, W. Theobald, P. K. Patel and F. N. Beg, submitted to J. Phys. Conf. Ser. IFSA 2015

<sup>26</sup> H. Shiraga, M. Heya, A. Fujishima, O.Maegawa et al., Rev. Sci. Instrum. 66, 722 (1995)

<sup>27</sup> H. Shiraga, S. Fujioka, P.A. Jaanimagi, C. Stoeckl, R.B. Stephens, H. Nagatomo, K.A. Tanaka, R. Kodama, and H. Azechi, Rev. Sci. Instrum. **75**, 3921 (2004).

M. Koga, Y. Ishii, T. Sogo, K. Shigemori, H. Shiraga, S. Fujioka, and H. Azechi, EPJ Web Conf. 59, 03006 (2013).
 G. Pretzier, H. Jger, T. Neger, H. Philipp, and J. Woisetschlger, "Comparison of Different Methods of Abel

<sup>29</sup> G. Pretzier, H. Jger, T. Neger, H. Philipp, and J. Woisetschlger, "Comparison of Different Methods of Abel Inversion Using Computer Simulated and Experimental Side-On Data," Zeitschrift fr Naturforschung, Vol. 47a, 1992, pp. 955–970.

<sup>30</sup> N. Ohnishi, High Energy Density Physics 8, 341-348 (2012).

<sup>31</sup> R. M. More, K. H. Warren, D. A. Young, and G. B. Zimmerman, Physics of Fluids 31, 3059-3078 (1988).

<sup>32</sup> J.J. MacFarlane, I.E. Golovkin, and P.R. Woodruff, J. Quant. Spectrosc. Radiat. Transf. 99, 381 (2006).

<sup>&</sup>lt;sup>20</sup> J. D. Lindl, Inertial Confinement Fusion (Springer, New York, 1998).

<sup>&</sup>lt;sup>21</sup> S. Atzeni and J. Meyer-ter-Vehn, The Physics of Inertial Fusion (Clarendon Press, Oxford, 2004).

<sup>&</sup>lt;sup>22</sup> C.D. Zhou, W. Theobald, R. Betti, P.B. Radha, V.A. Smalyuk, D. Shvarts, V.Y. Glebov, C. Stoeckl, K.S. Anderson, D.D. Meyerhofer, T.C. Sangster, C.K. Li, R.D. Petrasso, J.A. Frenje, and F.H. Seguin, Phys. Rev. Lett. 98, 025004 (2007).

<sup>&</sup>lt;sup>23</sup> S. Fujioka, T. Johzaki, Y. Arikawa, Z. Zhang, A. Morace, T. Ikenouchi, T. Ozaki, T. Nagai, Y. Abe, S. Kojima, S. Sakata, H. Inoue, M. Utsugi, S. Hattori, T. Hosoda, S.H. Lee, K. Shigemori, Y. Hironaka, A. Sunahara, H. Sakagami, K. Mima, Y. Fujimoto, K. Yamanoi, T. Norimatsu, S. Tokita, Y. Nakata, J. Kawanaka, T. Jitsuno, N. Miyanaga, M. Nakai, H. Nishimura, and H. Shiraga, 063102, 1 (2015).